MICROCOPY RESOLUTION TEST CHART
NATIONAL BUREAU OF STANDARDS-1963-A
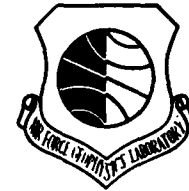
Test of an Inversion Algorithm for Spectrally Resolved Limb Radiance Profiles

A.S. ZACHOR
R.D. SHARMA

28 SEPTEMBER 1982

OPTICAL PHYSICS DIVISION   PROJECT 2310

AIR FORCE GEOPHYSICS LABORATORY
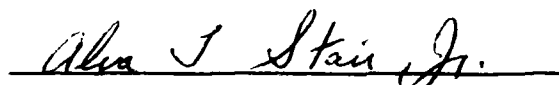
HANSCOM AFB, MASSACHUSETTS 01731

AIR FORCE SYSTEMS COMMAND, USAF

This report has been reviewed by the ESD Public Affairs Office (PA)
and is releasable to the National Technical Information Service (NTIS).

This technical report has been reviewed and
is approved for publication.

DR. ALVA T. STAIR, Jr
Chief Scientist

Qualified requestors may obtain additional copies from the
Defense Technical Information Center. All others should apply
to the National Technical Information Service.

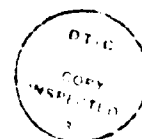| REPORT DOCUMENTATION PAGE		READ INSTRUCTIONS BEFORE COMPLETING FORM
1. REPORT NUMBER AFGL-TR-82-0280	2. GOVT ACCESSION NO. AD-A126	3. RECIPIENT'S CATALOG NUMBER 335
4. TITLE *(and Subtitle)* TESTS OF AN INVERSION ALGORITHM FOR SPECTRALLY RESOLVED LIMB RADIANCE PROFILES		5. TYPE OF REPORT & PERIOD COVERED Scientific. Interim.
		6. PERFORMING ORG. REPORT NUMBER PSRP No. 658
7. AUTHOR(s) A. S. Zachor* R. D. Sharma		8. CONTRACT OR GRANT NUMBER(s)
9. PERFORMING ORGANIZATION NAME AND ADDRESS Air Force Geophysics Laboratory (OPR) Hanscom AFB Massachusetts 01731		10. PROGRAM ELEMENT, PROJECT, TASK AREA & WORK UNIT NUMBERS 61102F 2310G415
11. CONTROLLING OFFICE NAME AND ADDRESS Air Force Geophysics Laboratory (OPR) Hanscom AFB Massachusetts 01731		12. REPORT DATE 28 September 1982
		13. NUMBER OF PAGES 20
14. MONITORING AGENCY NAME & ADDRESS(*if different from Controlling Office*)		15. SECURITY CLASS. *(of this report)* Unclassified
		15a. DECLASSIFICATION DOWNGRADING SCHEDULE

16. DISTRIBUTION STATEMENT *(of this Report)*

Approved for public release; distribution unlimited.

17. DISTRIBUTION STATEMENT *(of the abstract entered in Block 20, if different from Report)*

18. SUPPLEMENTARY NOTES This research was supported by Defense Nuclear Agency under subtask T25AAXHX63P, Work Unit 14, entitled "IR Data Evaluation of SIP2".

*Atmospheric Radiation Consultants, Inc., 59 High Street, Acton, MA 01720
Research supported under Contract F19628-81-C-0140

19. KEY WORDS

Limb radiance
Inversion algorithm
Spectrally resolved limb radiance profiles

20. ABSTRACT

Tests are described of a quasi-analytic algorithm that recovers vertical distributions of concentration and temperature by inversion of spectrally resolved limb radiance profiles. The tests, which used synthetic data...

Preface

The authors wish to thank Dr. A.T. Stair, Jr. of the Air Force Geophysics Laboratory for his interest and encouragement in this project.

Contents

Illustrations

Tests of an Inversion Algorithm for Spectrally Resolved Limb Radiance Profiles

I. INTRODUCTION AND SUMMARY

Spectrally resolved infrared radiance profiles of the Earth's limb can be inverted to obtain vertical distributions of temperature and species concentration. The atmosphere below approximately 70 km, where LTE prevails and the undissociated CO_2 distribution is kno , can be probed using broadband limb measurements, as demonstrated by House and Ohring,[1] Gille et al,[2] Russell et al,[3] and others. The added dimension of spectral resolution offers the potential of obtaining unambiguous information in the non-LTE altitude regime.

The limb spectral radiance profile cannot in general be expressed as a linear function of the vertical temperature and concentration profiles. Consequently, the inversion must generally be performed by some sort of recursive algorithm. Zachor et al[4] used a recursive direct nonlinear technique to recover vertical profiles of excited nitric oxide concentration and kinetic temperature above a 100-km altitude from spectral data measured by the rocket-borne SPIRE CVF spectrometer.[5,6] These inversions used SPIRE data for the NO fundamental band near 5.3 μm. Comparable results could have been obtained by an approximate linear method because ground state NO is optically thin for tangent paths above ~ 100 km

for the fundamental band. That is, the measured radiance profile and the excited state density profile have a relationship that is approximately linear for this special case. A nonlinear method can be adapted more easily to the general, non-optically-thin case, which is why we chose to use the nonlinear method in our earlier study,[4] referred hereafter to as ZSNS.

The direct nonlinear method starts with an initial guess for the solution profile, for example, the excited NO vertical density distribution. The corresponding limb radiance profile is computed and then the guess is relaxed according to some measure of the disagreement between the computed and measured limb radiance profiles. The relaxation equation used in the earlier study, Eq. (8) of ZSNS, revises the guess according to ratios of measured and computed radiance values. The process is iterated until the solution profile has converged.

The purpose of this study is to examine further the inversion capabilities of the relaxation method used in ZSNS, and to determine its sensitivity to noise. We were interested particularly in answering the following questions:

(a) How accurately can the method recover sharply-peaked distributions? In the limb viewing geometry, a layer far below the peak is observed through much denser layers above it.

(b) How accurately can the temperature profile be recovered when there is noise in the data? The temperature profile recovered in ZSNS had large, noise-like excursions.

These questions were answered by generating synthetic spectral limb radiance profiles and then inverting them, both before and after the addition of normally distributed pseudo-random numbers representing noise. We used the NO fundamental ($\Delta v = 1$) band and assumed that ground state NO is optically thin for the complete range of tangent paths involved in the simulations, which corresponded to tangent heights between 85 and 130 km. Thus, the equations used for the direct computation of radiance, spectral radiance and the relaxed guess are those given in ZSNS. The inversion method modified to handle the non-optically-thin case (and to recover ground state as well as excited state density) would be expected to have a slightly higher sensitivity to noise than will be indicated by the present results.

In the noise-free simulations, the excited NO vertical density profile was represented by a Gaussian function and also by a double-peaked distribution which is the sum of two Gaussians. The simulations with noise used only the double-peaked distribution. The added white spectral noise had two different rms levels, corresponding to maximum S/N's of 500 and 100; these are the signal-to-noise values at the combination of wavelength and tangent height that produces the maximum limb spectral radiance. The spectral resolution was the same as the SPIRE instrument, approximately 0.05 μm, which resolves the NO band into 13 spectral elements.

The excited NO density profile $NO^*(H)$ was retrieved by inverting the synthetic limb profile of band radiance (integrated spectral radiance), whereas the temperature inversion used 13 profiles of spectral radiance. As in the ZSNS study, the $NO^*(H)$ solution and the set of solutions obtained by inverting each spectral radiance profile are combined to obtain the profile $R(H, \lambda)$, the normalized spectral emission per unit volume as a function of altitude. The normalized spectral emission $R(T, \lambda)$ was also computed for various temperatures T. A systematic comparison of the retrieved $R(H, \lambda)$ and computed $R(T, \lambda)$s yields the temperature profile T(H). The initial guess in each of the inversions consisted of a constant (altitude-independent) value.

The results of the simulations are displayed in graphs in the following section. Examination of the results leads to the following conclusions:

(a) In the noise-free simulations the retrieved $NO^*(H)$ and T(H) were nearly identical to the models used to generate the synthetic limb radiance profiles, except at the very lowest altitudes, where the excited density was two orders of magnitude lower than the peak value(s). The errors at the low altitudes are very likely due to the fact that the synthetic radiances were inadvertently rounded to four significant figures. (See Figures 3-5 in Section 3.)

(b) For $(S_\lambda N_\lambda)_{peak} = 500$, the excited NO density can be retrieved with high accuracy down to density levels 50 times smaller than the peak. Below this density level, the accuracy degrades rapidly. It appears that the inversion technique we have used is no less accurate at altitudes below the lower NO^* peak than it is above the higher NO^* peak, although the errors tend to be more systematic in the lower altitude range (see Figure 6).

(c) For $(S_\lambda N_\lambda)_{peak} = 100$ the errors in retrieved NO^* density profile have the same behavior as for the higher S/N case, except that the retrieved profile is accurate to levels 20 times lower than the peak (see Figure 7).

(d) The accuracy of retrieved translational temperature degrades rapidly above some upper altitude limit and below some lower limit. However for $(S_\lambda N_\lambda)_{peak} = 500$ the rms error in T(H) is less than approximately $10°C$ over a wide range of altitudes. For $(S_\lambda N_\lambda)_{peak} = 100$, the rms error is about $10-20°C$ near the NO^* peaks; the errors become larger than $50-75°C$ very rapidly as the actual NO^* decreases to less than one-tenth the NO^* peak value (see Figures 8 and 9).

(e) Examination of the results indicates that the random peak
excursions in the retrieved temperature profile at the altitudes
of the NO^* peaks are approximately $\pm 5°C$ for maximum spectral
S/N = 500 and approximately $\pm 25°C$ for $(S_\lambda/N_\lambda)_{max}$ = 100. The
temperature profile that we retrieved from the SPIRE NO data
(see ZSNS) has excursions of $\pm 75°C$ near the altitude of
maximum NO^*, approximately 130 km. This would be consistent
with the present simulation results if the spectral signal-to-noise
of the SPIRE data for tangent height H_T = 130 km was approxi-
mately 30 (after the data is averaged over 0.05 μm intervals,
as done by ZSNS). Examination of the SPIRE data for this
tangent height shows that the enhanced S_λ/N_λ is somewhat
greater than 30, but probably not more than 60. Hence, the
present results support the conclusions by ZSNS that detector
noise was the major cause of the noise-like excursions in the
temperature profile retrieved from the SPIRE NO data.

(f) The results emphasize the importance of achieving high signal-
to-noise in limb spectral radiance measurements, and also
of considering the tradeoffs between spectral resolution and
signal-to-noise. This study did not consider the effects of
smoothness constraints on the inversion solutions, which might
reduce considerably the S/N requirement.

2. RESULTS OF SIMULATION

The single-peaked Gaussian distribution used to represent the excited density
profile $NO^*(H)$ in the simulations is given by

$$NO^*(H) = 5 \times 10^4 \exp \left[(H-115)/5 \right]^2 , \tag{1}$$

where NO^* has the units cm^{-3} and the altitude H is in kilometers. The density
profile peaks at 115 km and is e^{-1} times the peak value at 110 and 120 km altitude.
The double-peaked distribution, given by

$$NO^*(H) = 5 \times 10^4 \left\{ \exp \left(\left[(H-115)/4.3437 \right]^2 \right) \right.$$
$$\left. + \exp \left(\left[(H-100)/4.3437 \right]^2 \right) \right\} , \tag{2}$$

has a relative minimum at 107.5 km, where NO^* is approximately one-tenth the
maximum value $(\sim 5 \times 10^4 \ cm^{-3})$ which occurs at 100 km and 115 km.

10

The translational temperature profile used in the computation of synthetic radiances is the profile given by the Jacchia[7] model for an exospheric temperature of 1050K (based on the U.S. Standard Atmosphere 1976). The profile is displayed in graphs that compare the model T(H) to the inversion results, which are described below. Figures 1 and 2 show the two different $NO^*(H)$ models and the corresponding computed limb profiles of band radiance. The 13 computed limb spectral radiance profiles are not shown.

Figure 3 compares the single-peaked "actual" or model NO^* distribution and the corresponding retrieved profile when no noise has been added to the synthetic band radiance profile. However, the synthetic band radiances were rounded to four significant figures before they were inverted. Note that the error is significant only at the lowest altitudes, where $NO^*(H)$ is less than 0.01 times the peak NO^*. Figure 4 shows that the error has essentially the same behavior for the double-peaked case.
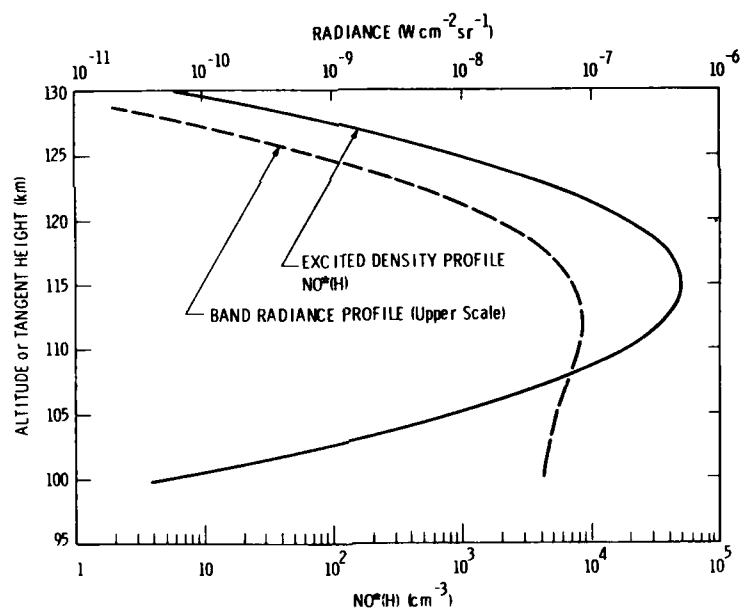

Figure 1. Single-peaked Gaussian Model for $NO^*(H)$ and the Limb Profile of Band Radiance, Determined by $NO^*(H)$ and the Model Temperature Profile T(H)

7. Jacchia, L. (1977) Thermospheric Temperature, Density and Composition: New Models, Smithsonian Astrophysical Observatory Special Report 375.
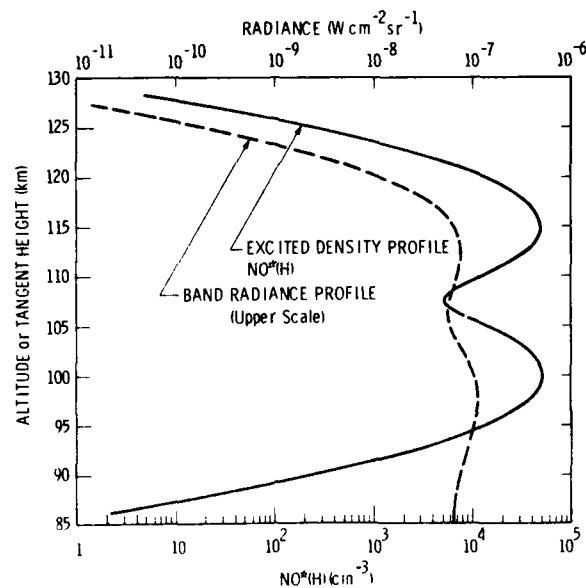
Figure 2. Same as Figure 1, Except the Model for $NO^*(H)$ Is the Sum of Two Displaced Gaussian Functions

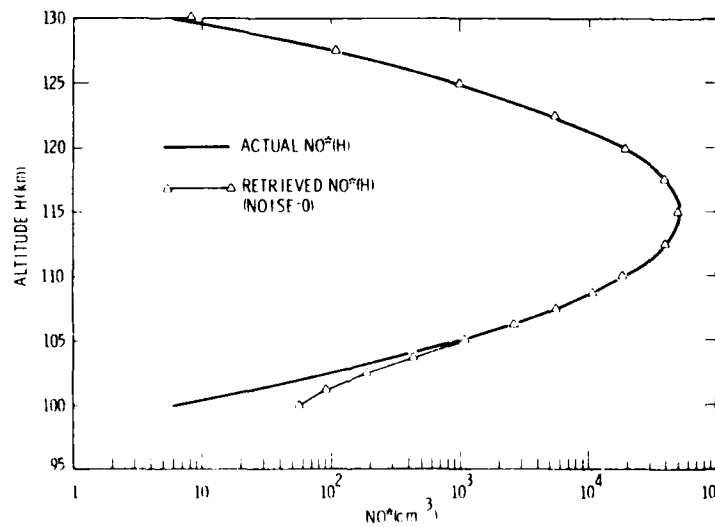Figure 3. Actual and Retrieved Excited Density Profiles $NO^*(H)$ for the Noise-free Case. However, the synthetic limb radiance profile was rounded to four significant figures
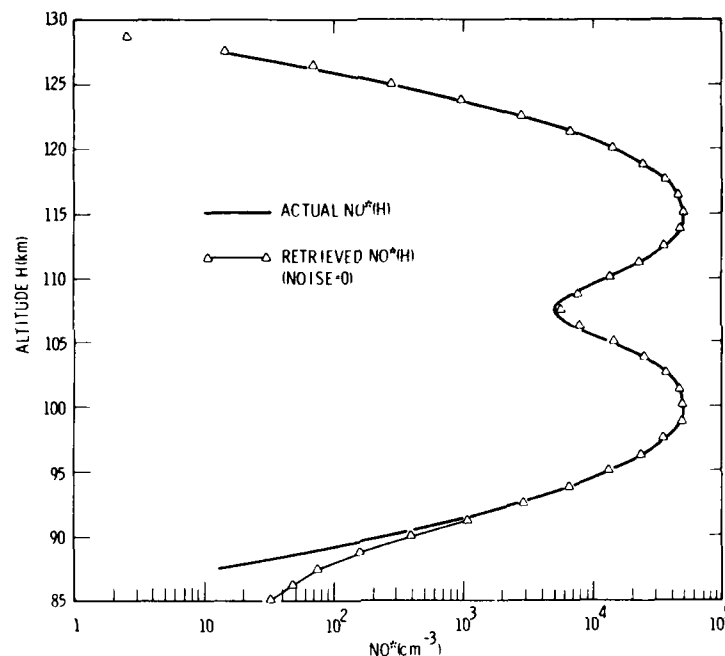
Figure 4. Same as Figure 3 Except that the Actual
$NO^*(H)$ Is Represented by the Double-peaked Model

Figure 5 compares the actual or model T(H) to the temperature profiles re-
trieved for the single- and double-peaked cases, when only rounding noise is
present. The errors in retrieved T(H) are significant at the same altitudes for
which the retrieved $NO^*(H)$ has significant errors, that is, when $NO^*(H)$ is less
than 0.01 times the peak NO^*.

Figure 6 shows the retrieved double-peaked NO^* vertical profile when the
maximum spectral S/N is 500. The retrieved profile is in good agreement with
the actual profile when $NO^*(H)$ is greater than ~0.01 to 0.02 times the peak NO^*.
For a maximum spectral S/N of 100 the actual and retrieved profiles are in good
agreement when $NO^*(H)$ is greater than approximately 0.02 times the peak NO^*;
see Figure 7. However, at 107.5 km where NO (H) has a relative minimum, the
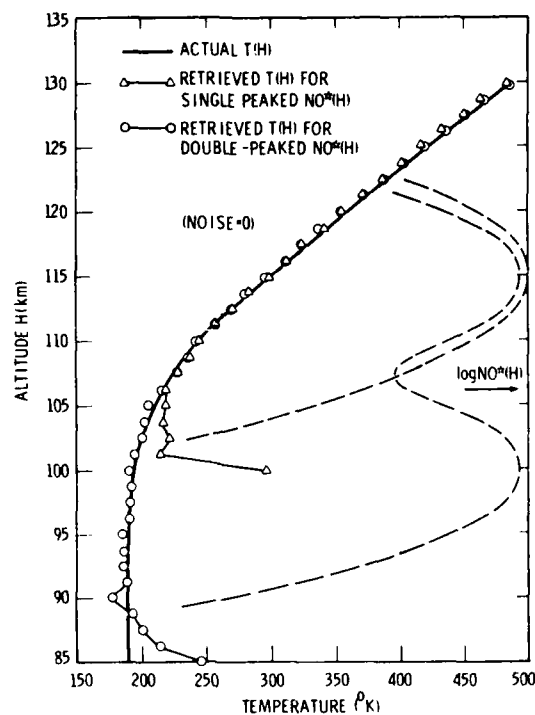relative error is approximately 40 percent.

Figure 5. Actual and Retrieved Temperature Profiles. The retrieved profiles are shown for both single-peaked NO* and Double-peaked NO*

Figure 8 shows that accurate temperature profiles can be retrieved over the range of altitudes corresponding to NO*(H) $\gtrsim$ 0.10 NO*$_{peak}$ when $(S_\lambda/N_\lambda)_{max}$ = 500. For the double-peaked model used in the simulations this altitude range is approximately 95-120 km; the error in this altitude regime is less than ~20°C.

Figure 9 shows that the retrieved profile has unacceptably large errors when $(S_\lambda/N_\lambda)_{max}$ ~ 100. The rms error in temperature is less than ~10-20°C only near the peaks of the NO* distribution.
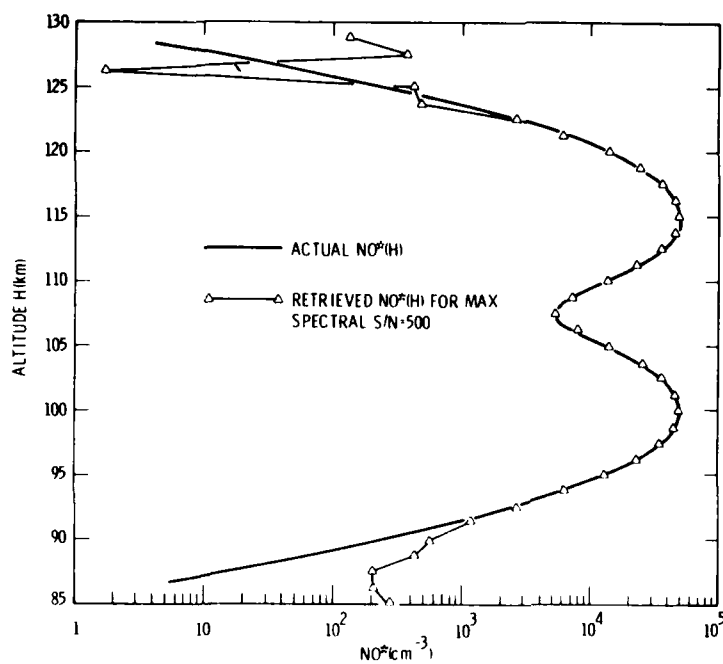
Figure 6. Actual and Retrieved Density Profiles $NO^{*}(H)$ for $(S_{\lambda}/N_{\lambda})_{max} = 500$, Double-peaked Case
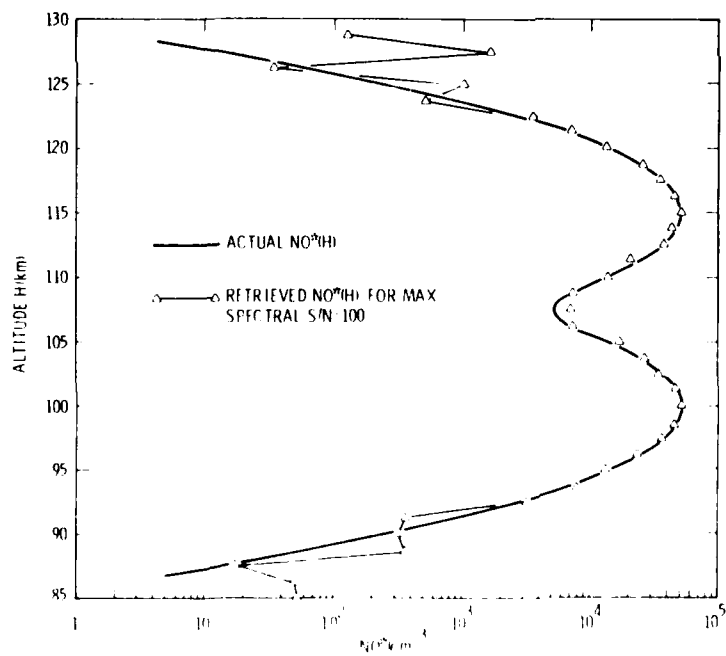

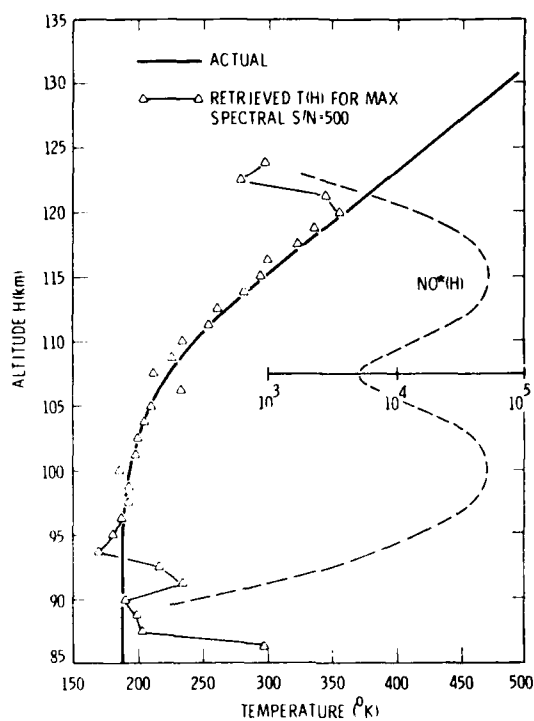Figure 7. Same as Figure 6, Except $(S_{\lambda}/N_{\lambda})_{max}$ 100

16

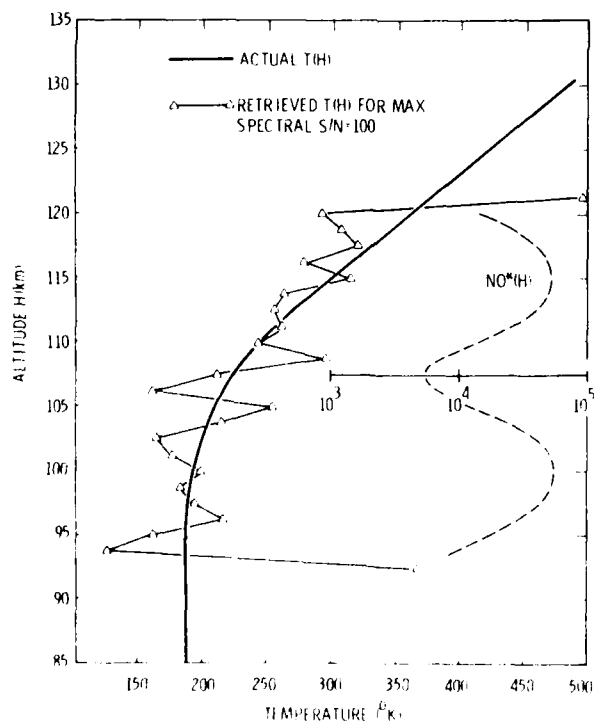Figure 8.   Retrieved Temperature Profile for $(S_\lambda/N_\lambda)_{max} = 500$, Double-peaked Case

Figure 9.   Same as Figure 8, Except $(S_\lambda/N_\lambda)_{max} = 100$

3. DISCUSSION

It appears that the nonlinear inversion technique investigated in this study is no less accurate below the peak(s) in concentration distribution than it is above the peak(s), although the errors tend to be more systematic at the lower altitudes below a single or double peak.

Based on the results of this study, it is not surprising that the temperature profile retrieved from the SPIRE NO spectral data by ZSNS show noise-like excursions of $\pm 75°C$. The maximum S_λ/N_λ was between 30 and 60 for the SPIRE data. The present study implies that maximum spectral S/Ns of the order of 500 are required to ensure acceptable temperature solutions.

Translational temperature profiles in the thermosphere have a characteristic smoothness exemplified by the model T(H) used in the simulations. Based on the a priori knowledge (or assumption) of "smoothness", the retrieved temperature profile shown in Figure 9 would be judged "unacceptable". So-called smoothness constraints can be incorporated into the inversion algorithm to significantly reduce the S/N requirement. For the double-peaked NO cases modelled in this study, it is estimated that the S/N requirement can be reduced by a factor as large as two or three.

The study results indicate, nonetheless, the importance of considering the available tradeoffs between spectral resolution and signal-to-noise. High spectral resolution might be required, for example, when two or more species have overlapping spectral bands, or when the available data interpretation algorithm requires isolation of optically-thin portions of a strongly emitting band. When these conditions do not apply one should opt for the minimum spectral resolution that resolves the band contour (translational temperature). The tradeoffs obviously become more complex when the instrument must recover simultaneously the distributions of several species.

References

1. House, F. B., and Ohring, G. (1969) Inference of Stratospheric Temperature and Moisture Profiles from Observations of the Infrared Horizon, NASA CR-1419, GCA Corp., Bedford, Massachusetts.

2. Gille, J.C., Bailey, P.L., Craig, R.A., and Thomas, J.R. (1975) The limb radiance inversion radiometer (LRIR) experiment, in the Nimbus 6 Users Guide, Goddard Space Flight Center, J.E. Sissola, ed., p. 141.

3. Russell, J.M., III, Gille, J.C., Gordley, L.L., and Remsberg, E.E. (1979) The Limb Infrared Monitor of the Stratosphere (LIMS) Experiment: H$_2$O, NO$_2$, and HNO$_3$ Results, Proceedings of the IAMAP Symposium, Seventeenth General Assembly of the IUGG, 2-15 Dec., 1979, Canberra, Australia.

4. Zachor, A.S., Sharma, R.D., Nadile, R.M., and Stair, A.T., Jr. (1981) Inversion of SPIRE NO Data, AFGL-TR-81-0325, AD A108366.

5. Nadile, R.M., et al. (1981) SPIRE - Spectral infrared rocket experiment, Proc. Soc. Photo-Opt. Instr. Eng., 245:148.

6. Stair, A.T., Jr., et al. (1985) Infrared radiometric measurements of Aurora, Airglow, and the upper atmosphere, IAMAP/ICMUA Symposium 5, Kyoto, Japan, S. ... , Atmospheric Aeronomy.

7. Grieder, W. (1981) Low Light Level Television System Design for the OSO New Mexico, Southwest Astronomy and Astrophysics Observatory, SWR-AR Report 71.

Air Force Geophysics Lab (AFGL)
Hanscom AFB, MA 01731
    Attn: R. Armstrong
            W. Blumberg
            R. Davis
            H. Gardiner
            R. Huffman
            A. McIntyre
            R. Murphy
            R. Nadile
            R. O'Neil
            R. Philbrick
            B. Sanford
            R. Sharma
            A. T. Stair

Air Force Office of Scientific Research
(AFOSR) Bolling AFB,
Washington, DC 20332
    Attn: D. Ball
            T. Cress

Air Force Space Division
P.O. Box 92960
Worldway Postal Center
Los Angeles, CA 90009
    Attn: R. Chadbourne
            T. May

Air Force Technical Applications Center
(AFTAC) Patrick AFB, FL 32925
    Attn: R. Bigoni

Air Force Weapons Lab (AFWL)
Kirtland AFB, NM 87117
    Attn: J. Mayo

Defense Nuclear Agency
Washington, DC 20305
    Attn: C. Fitz
            P. Lunn
            W. McKechney

Aerospace Corp.
P.O. Box 92957
Los Angeles, CA 90009
    Attn: J. Cresswell
            P. Kislink
            I. Simmons
            I. Stocker
            L. Spiro
            R. Hope
            G. Light

Electrodynamics Laboratory
Utah State University
Logan, UT 84322
    Attn: D. Baker
            A. Steed
            C. Wyatt

General Research Corp.
Santa Barbara, CA 93111
    Attn: J. Ise

General Electric Tempo
816 State Street (PO Drawer QQ)
Santa Barbara, CA 93102
    Attn: T. Stephens

Lockheed Missiles and Space Co., Inc.
3251 Hanover Street
Palo Alto, CA 94304
    Attn: J. Kumer
            R. Sears

Mission Research Corp.
P. O. Drawer 719
Santa Barbara, CA 93102
    Attn: D. Archer
            D. Sappenfield

Photometrics Inc.
7 Arrow Way
Woburn, MA 01801
    Attn: G. Davidson
            I. Kovsky

Physical Sciences Inc.
30 Commerce Way
Woburn, MA 01801
    Attn: G. Caledonia

R&D Associates
P.O. Box 9695
Marina Del Ray, CA 90291
    Attn: F. Gilmore

Space Measurements Lab
Utah State University
Logan, UT 84322
    Attn: K. Baker
            D. Burt

Space Data Corp.
1333 West 21st Street
Tempe, AZ 85282
    Attn: S. Fisher
            D. Kush

19

Stewart Radiance Lab
Utah State University
Bedford, MA 01730
    Attn: R. Huppi
            J. Ulwick

SRI International
333 Ravenswood Ave.
Menlo Park, CA 94025
    Attn: W. Chesnut

Visidyne, Inc.
5 Corp. Place, S. Bedford St.
Burlington, MA 01803
    Attn: J. Carpenter
            T. Degges
            C. Humphrey
            W. Reidy
            H. Smith

4-8

DTI